FLORIDA DEPARTMENT OF TRANSPORTATION

Experimental Investigation of the Effect of Surface Markings on the Mechanical Integrity of Weathering Bridge Steels - Phase III
Final Report

FDOT BDV31-977-84

February 2018

University of Florida, Department of Materials Science and Engineering
Dr. Michele V. Manuel, Chair and Professor

DISCLAIMER PAGE

The opinions, findings, and conclusions expressed in this publication are those of the authors and not necessarily those of the State of Florida Department of Transportation.

METRIC CONVERSION CHART

Conversion to SI units

SYMBOL	WHEN YOU KNOW	MULTIPLY BY	TO FIND	SYMBOL
LENGTH				
mil	Thousandth of an inch	0.0254	millimeters	mm
in	inches	25.4	millimeters	mm
ft	feet	0.305	meters	m
yd	yards	0.914	meters	m

SYMBOL	WHEN YOU KNOW	MULTIPLY BY	TO FIND	SYMBOL
AREA				
in^2	square inches	645.2	square millimeters	mm^2

SYMBOL	WHEN YOU KNOW	MULTIPLY BY	TO FIND	SYMBOL
MASS				
lb	pounds	0.454	kilograms	kg

SYMBOL	WHEN YOU KNOW	MULTIPLY BY	TO FIND	SYMBOL
TEMPERATURE (exact degrees)				
^oF	Fahrenheit	5 (F-32)/9 or (F-32)/1.8	Celsius	^oC

SYMBOL	WHEN YOU KNOW	MULTIPLY BY	TO FIND	SYMBOL
FORCE and PRESSURE or STRESS				
lbf	poundforce	4.45	newtons	N
lbf/in^2	poundforce per square inch	6.89	kilopascals	kPa
ksi	kilopound per square inch	6894.75	kilopascals	kPa

APPROXIMATE CONVERSIONS TO SI UNITS

SYMBOL	WHEN YOU KNOW	MULTIPLY BY	TO FIND	SYMBOL
LENGTH				
mm	millimeters	0.039	inches	in
m	meters	3.28	feet	ft

SYMBOL	WHEN YOU KNOW	MULTIPLY BY	TO FIND	SYMBOL
AREA				
mm^2	square millimeters	0.0016	square inches	in^2
m^2	square meters	10.764	square feet	ft^2

SYMBOL	WHEN YOU KNOW	MULTIPLY BY	TO FIND	SYMBOL
MASS				
g	grams	0.035	ounces	oz
kg	kilograms	2.202	pounds	lb

*SI is the symbol for the International System of Units. Appropriate rounding should be made to comply with Section 4 of ASTM E380.

Technical Report Documentation Page

1. Report No.	2. Government Accession No.	3. Recipient's Catalog No.

4. Title and Subtitle	5. Report Date
Experimental Investigation of the Effect of Surface Markings on the Mechanical Integrity of Weathering Bridge Steel – Phase III	February 2018
	6. Performing Organization Code
7. Author(s) Dr. Michele V. Manuel	8. Performing Organization Report No.
9. Performing Organization Name and Address University of Florida 100 Rhines Hall 549 Gale Lemerand Drive Gainesville, Florida 32611	10. Work Unit No. (TRAIS)
	11. Contract or Grant No. BDV31-977-84
12. Sponsoring Agency Name and Address Florida Department of Transportation 605 Suwannee Street, MS 30 Tallahassee, FL 32399	13. Type of Report and Period Covered Final Report October 2017 – January 2018
	14. Sponsoring Agency Code

15. Supplementary Notes

16. Abstract

The purpose of this work was to study the effect of (1) marking parameters – head speed (writing) and amperage (current) – on the plasma notch and heat affected zone (HAZ) depth and (2) the plasma notch and HAZ depth on the mechanical properties of 50W weathering bridge steel. Both marking parameters will be altered, resulting in varying plasma notch and HAZ depth. A relationship between plasma marking parameters and notch HAZ depth will be revealed, as well as its consequent effects on the fatigue life. The overall goal of this study was to provide guidelines for marking bridge steels for future standardization and implementation.

17. Key Word	18. Distribution Statement
Fatigue, Weathering Steel, 50W, Plasma Marking	No restrictions

19. Security Classif. (of this report)	20. Security Classif. (of this page)	21. No. of Pages	22. Price
Unclassified	Unclassified	37	

Executive Summary

Currently, the bridge steel industry relies on time consuming manual methods for marking rolled steel plates during the production process. These markings are necessary for labeling welding positions, plate orientation, and part identification. Recently, the steel industry is looking for automated methods such as plasma marking as alternative to the traditional manual marking methods. The purpose of this work was to study the effect of (1) plasma marking parameters – head speed (writing) and amperage (current) – on the notch and heat affected zone (HAZ) depth done during the marking process and (2) the notch and HAZ depth on the mechanical properties of 50W weathering bridge steel.

A set of thirteen 50W high strength low alloy (HSLA) weathering steel plates were acquired from Tampa Tank Structural Steel Inc. These steel plates were marked using different marking parameters, resulting in varying notch and HAZ depths. To determine the correlation between marking parameters and the notch and HAZ depths three plates were marked using currents ranging from 10 to 15A at marking speeds between 100 and 250 in/min. After measuring the notch and HAZ depths of samples obtained from these plates it was shown that the current has an effect on notch and HAZ depth while head speed was shown to create no change in the HAZ depth in a consistent or predictable manner. The analysis was based on detailed microstructural characterization and statistical analysis. To study the effect of these notch and HAZ depth on the mechanical properties of the 50W grade steel plasma marked, tensile strength and fatigue life measurements were carried out. After testing tensile specimens marked at 15 A and 75 in/min it was concluded that there is a minimal effect of the marking on the tensile strength of the material at the marking condition of 15 A. In the other hand, a considerable number of specimens marked using the same conditions experienced failure at the plasma mark. The minimum fatigue life obtained was 107,458 cycles which is considerably lower than the minimum fatigue lifetime required for 50W structural steel bars. Fatigue testing was also performed to samples plasma marked with a current of 10 A at 150 in/min speed. The samples do not seem to be weakened by the plasma mark (e.g., low number of samples failed below the AASHTO Category A limit). After testing a total of 108 samples plasma marked using a current of 10 A it was determined that there is only a 3.2% probability of the sample failing below the AASHTO minimum fatigue lifetime for 50W steel, category A.

The 10-A condition creates a visible and robust mark that can be used for surface marking. Although there is a 3.2% probability that a sample marked with plasma at a current of 10 A and 75-250 in/min speed will fail below the AASHTO minimum fatigue lifetime for 50W grade steel, the minimum fatigue life obtained was 170,767 cycles which is considerably close to the minimum fatigue lifetime required for 50W structural steel bars. This study has shown that this technology has the potential to be used as an automatic technique for marking 50W grade steel.

Table of Contents

1 Introduction 1

2 Methods 2

3 Results and Discussion 5

3.1 Notch and HAZ Depth Measurements of Samples Plasma Marked at Different Marking Parameters 5

3.1.1 Correlation Between Marking Parameters and Notch and HAZ Depths 5

3.1.2 Comparison of Notch and HAZ Depths Among Plates 8

3.1.3 Changes in Notch and HAZ Depth Along the Plasma Marks 11

3.2 Mechanical Characterization 12

3.2.1 Tensile Testing of Marked Specimens 12

3.2.2 Fatigue Life of Specimens Marked at Different Parameters 13

3.3 Fatigue Life Probability Plots 17

4 Final Safety Guideline Result 19

5 Summary 20

References 21

Appendix A 22

List of Figures

Figure 2-1. Tensile specimen geometry with dimensions in inches. 3
Figure 2-2. KB fatigue specimen geometry. Dimensions shown in inches. 3
Figure 3-3. Micrograph showing the scribe mark and the associated HAZ. 5
Figure 3-4. Average HAZ depth as function of amperage at discrete marking speeds (Plate A). 6
Figure 3-5. Contour plot indicating trends in absolute values of HAZ depth as a function of current and head speed (Plate A). 7
Figure 3-6. Contour plot indicating trends in absolute values of notch and HAZ depths as a function of current and head speeds of Plate B (left) and Plate C (right). 8
Figure 3-7. Comparison of HAZ depth among plate A, B and C (B+C) for 15 A and 250 in/min. The box indicates the interquartile range. Error bars represent 1st (upper) and 3rd (lower) quartile. 9
Figure 3-8. Micrograph of Plate C (500X). 10
Figure 3-9. Plasma marks at 13 A and 175 in/min setting (above) and 10 A and 250 in/min setting (below) 11
Figure 3-10. HAZ depth trails off as mark continues (above) and associated distances (below). Marked at 15 A and 250 in/min 12
Figure 3-11. Representative stress versus strain curve illustrating the mechanical properties for bulk failure of tensile specimen. 13
Figure 3-12. Stress range as function of number of cycles for the plate marked at 15 A, 75 in/min. Points in red represent samples that failed at the plasma mark. The fatigue data is overlaid on the AASHTO standard, where the black line represents Category A guidelines 14
Figure 3-13. Scatter plot of cycles to failure vs. HAZ depth. Points in red indicate samples that failed at the HAZ. Light red zone indicates the range of HAZ depths that could cause premature to minimum fatigue life failure. 15
Figure 3-14. Stress range vs. cycles to failure for 50W samples marked at the 10-A condition. (a) Data from all plates marked at three different head speeds, (b). Plates 9 and 10 marked at 75 in/min, (c) Plates 4, 5, and 6 marked at 150 in/min, and (d) Plates 7 and 8 marked at 250 in/min. In every plot, the samples that failed in the plasma mark are identified by the color orange. 16
Figure 3-15. Normal distribution plot showing probability of failure below minimum fatigue life of 175,000 cycles for samples marked at 10 A and head speeds of (a) 75, (b) 150, (c) 250 in/min, and (d) all conditions. The minimum life according to the AASHTO guidelines is indicated by the red dotted line. 18
Figure A-16. Micrograph at 500x for plate A (top), and plate B (bottom). 23

List of Tables

Table 2-1. Summary of the plates used in this study and the respective marking parameters. ... 4
Table 3-1. Descriptive t-test statistics with a significance level of p set at 0.05. ... 8
Table 3-2. T-test results of the plates showing plate A having a statistically different notch and HAZ depth relative to plates B+C ... 9
Table 3-3. Grain sizes of plates A, B, C and 50W weathering steel. ... 10
Table 3-4. Average Vickers hardness values of plates A, B, and C, using a 500-gram force. ... 10
Table 3-5. Average number of cycles to failure of the tested plates and marking conditions. ... 17
Table A-1. Project Schedule ... 22
Table A-2. Ultimate tensile strength and yield strength values for specimens from plate 1 and 3. ... 24
Table A-3. Cycles to failure (fatigue life) of specimens from plates 1-3. ... 25
Table A-4. Cycles to failure (fatigue life) of specimens from plates 4-10 ... 26

1 Introduction

Currently, the bridge steel industry relies on manual methods of marking rolled steel plates during the production process (AASHTO 2015). These markings are necessary for labeling welding positions, plate orientation, and part identification. The process consists of manually measuring for marking positions on a plate, then die stamping or spray painting to make a mark. This procedure is time consuming and can result in the loss of markings during subsequent manufacturing processes. The industry is looking to advanced marking techniques, such as plasma marking, in order to enhance production efficiency (Faulkner 2011). The depth at which these techniques etch the surface needs to be controlled in order to preserve structural integrity over the predicted lifetime of the member. Previous work by (Kesler et al. 2016) has shown that relatively shallow markings with depths of up to 12 mils (300 μm) on 0.25" 50W steel result in negligible effects on fatigue life. Additionally, of the three techniques studied, which included mechanical milling, plasma, and laser marking, plasma marking left the most significant mark and, thus, would have the greatest effect on fatigue life. Plasma marks have two controlling parameters, which include the amperage/current setting of the machine, which ranges from 5-15 Amperes (A), and head speed, which reaches speeds of up to 400 inches per minute. Varying these parameters will result in a range of plasma mark depths and heat damage on the surface of the steel plates and, thus, may result in diminished fatigue life. This research program investigates the safe limits of plasma marking depth on a 50W weathering steel. Through a systematic study, the plasma marking parameters will be related to the marking depth and fatigue life.

This report discusses the effect of plasma marking parameters on the notch and HAZ depths created by the plasma marking on 0.5" 50W bridge steels. The analysis was based on detailed microstructural and mechanical property characterization and statistical analysis. The underlying goal of this work was to provide safe marking guidelines for marking bridge steel components. These analyses produced guidelines that can help to determine the marking parameters that would create a visible mark while not affecting the tensile and fatigue properties of the material.

2 Methods

Thirteen 18”x18”x0.5” plates of grade 50W high strength low alloy (HSLA) weathering steel were acquired from Tampa Tank Structural Steel Inc. The plates used to study the effect of marking parameters on notch and HAZ depths were designated A, B, and C, and the plates used for mechanical testing were numbered 1 through 10. Plates 1, 2, and 3 were cut from one bridge member, while plates 4-6 were cut from a separate member, and 7-10 were cut from a third member.

The plasma marking was carried out using the Messer Cutting Systems Oxy/Plasma Cutter/Writer that is in use for cutting and marking weathering steel at Tampa Tank Structural Steel. This system is typically used for sectioning and cutting plates using a current of 200 amperes (A). By limiting the current to 8-15 A, plates can be surface marked. Tampa Tank Structural Steel marked several plates at chosen marking parameters. Prior to marking, the plates were sandblasted, and following the plasma marking, they were then weathered to simulate the procedure used by Tampa Tank Structural Steel on large bridge members. Plates 1 to 10 were then transported to MTE Inc. in Gainesville, Florida to have mechanical testing samples sectioned from the plates using electrical discharge machining (EDM).

After sandblasting, marking, and weathering, a LECO MSX205M cut-off saw was used to make specimens for optical imaging of plate microstructure and HAZ. Samples were obtained from the entire the plate. These samples were then mounted in epoxy and polished using silicon carbide grinding papers of grits 120, 320, 600, 800, and 1200. Final polish was completed using a 1µm alumina slurry. Etching was performed using Nital (3% nitric acid, 97% ethanol) solution to reveal the microstructure. Optical imaging of the HAZ was performed using a Keyence VHX900F optical microscope. Grain size measurements were performed using linear intercept method and averaged by taking five measurements in accordance to specifications set out in ASTM E112 (ASTM 2013). Hardness testing was performed using a 500 gram-force, on a Wilson Hardness Tukon 1102 Hardness Tester with a Vickers indenter in accordance with ASTM standards for rolled structural steel(ASTM 2016).

To study the relation between the marking parameters and the notch and HAZ depths, plates A, B and C were marked using currents ranging from 10 to 15 A at marking speeds between 100 and 250 in/min. Table 2-1 shows the details of marking parameters used to mark each of the plates. For tensile testing, plates 1 and 3 were marked using a currents values of 10, 13 and 15 A at a speed of 75 in/min (Table 2-1). Samples were obtained from different positions on the plate to account for differences in yield strength that can be created across the plate width during rolling. Tensile samples were prepared following the geometry for a 0.5” plate in accordance with ASTM E8/E8M(ASTM 2009). This geometry is shown below in Figure 2-1. The tensile specimens were tested in an Instron 5582 load frame using mechanical wedge grips.

Yield and ultimate strength values were determined according to ASTM E8/E8M (ASTM 2009). A total of 15 samples were tested.

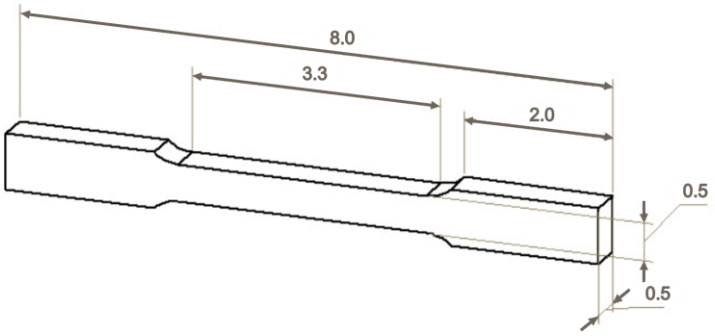

Figure 2-1. Tensile specimen geometry with dimensions in inches.

For fatigue testing, plate 2 was marked using a current of 15 A at a speed of 75 in/min, plates 4 to 6 were marked with a current of 10 A at 150 in/min, plates 7 and 8 with a current of 10 A at 250 in/min and plates 9 and 10 with a current of 10 A at 75 in/min (Table 2-1). A KB bar specimen geometry was used for fatigue specimens due to the irregular geometry of the plasma mark and the existence of a notch and HAZs rather than a direct machined notch (Bain and Miller 2000). This geometry is shown below in Figure 2-2. Each fatigue specimen sample was run at a specific stress range below the yield stress of the material (e.g. high cycle fatigue), to create a stress range vs. cycles to failure plots. Fatigue samples were tested in an MTS 470 with hydraulic wedge grips. In fatigue, 33 samples were tested at 15 A and 108 samples were tested at 10 A (a total of 141 samples). Samples were tested at a stress amplitude of 50 ksi, with an R value of 0.1. A frequency of 26-33 Hz was used for testing. After fatigue testing, notch and HAZ depths were measured (on the same plate that the specimen originated from) in order to identify the effect of notch and HAZ depths of each specimen on its fatigue life (cycles to failure).

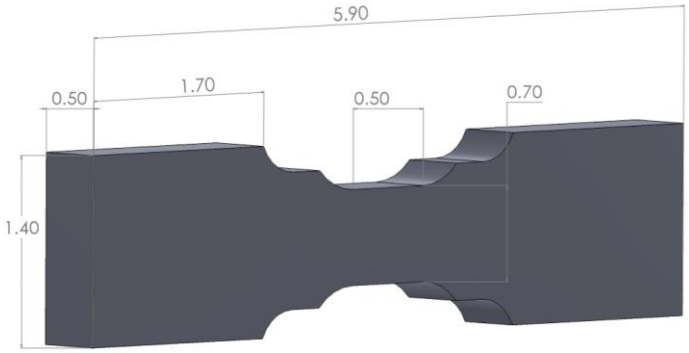

Figure 2-2. KB fatigue specimen geometry. Dimensions shown in inches.

Table 2-1. Summary of the plates used in this study and the respective marking parameters.

Plate Name	Marking Parameters		Characterization
	Current (A)	Head speed (in/min)	
A	10, 13, 15	100, 150, 250	HAZ
B	13, 15	100, 150, 250	HAZ
C	13, 15	100, 150, 250	HAZ
1	10, 13, 15	75	Tensile Strength
2	15	75	Fatigue Life
3	15	75	Tensile Strength
4	10	150	Fatigue Life
5	10	150	Fatigue Life
6	10	150	Fatigue Life
7	10	250	Fatigue Life
8	10	250	Fatigue Life
9	10	75	Fatigue Life
10	10	75	Fatigue Life

Statistical analysis of the effect of marking parameters on notch and HAZ depths was completed using an analysis of variance (ANOVA) method. Tukey and t-tests were done to determine statistical differences between plates with the Minitab software program. A significance level of 0.05 was set for the ANOVA and t-tests. Statistical analysis of fatigue results was completed using ANOVA method to study the influences of the current and head speed on the fatigue life of the marked specimens. Normal probability plots were created to determine the probability of a sample failing below the minimum established by American Association of State Highway and Transportation Officials (AASHTO) for 50W steel.

3 Results and Discussion

3.1 Notch and HAZ Depth Measurements of Samples Plasma Marked at Different Marking Parameters

3.1.1 Correlation Between Marking Parameters and Notch and HAZ Depths

The effect of marking parameters on the notch and HAZ depth was studied. Figure 3-3 shows a typical optical micrograph of the plasma mark. All the notches and HAZ reported measurements were obtained as illustrated in Figure 3-3. For simplification these depth measurements (notch+HAZ) will be called HAZ through the report.

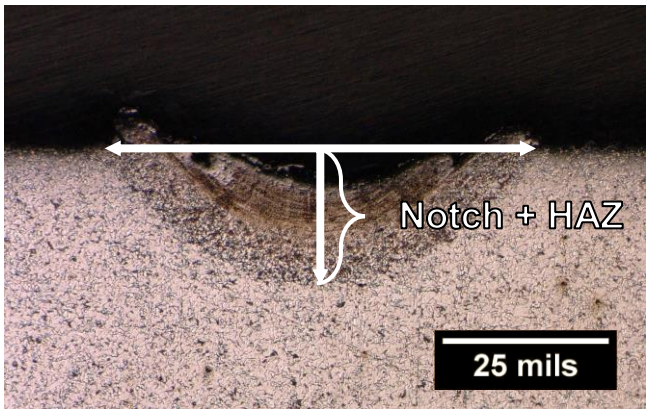

Figure 3-3. Micrograph showing the scribe mark and the associated HAZ.

Figure 3-4 shows the effect of head speeds on the notch and HAZ depths as a function of the current. Each data point represents an average of five measurements with the error bar representing one standard deviation. The data showed an increase in the notch and HAZ depths as a function of current between 10 and 13 A, but this trend differs at higher current levels. There is a large amount of variability at the 13 and 15 A current levels, as shown by the magnitude of the error bars (standard deviations) in Figure 3-4.

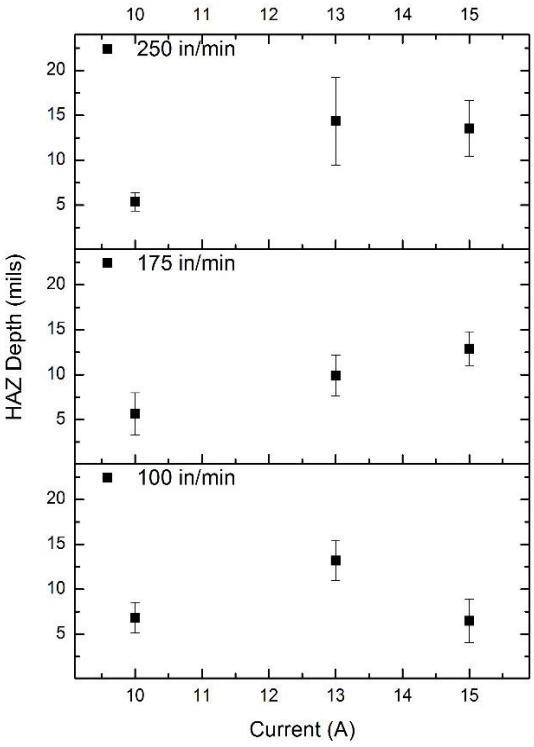

Figure 3-4. Average HAZ depth as function of amperage at discrete marking speeds (Plate A)

The contour plot shown in Figure 3-5 indicates trends in absolute values of notch and HAZ depths as a function of both current and head speed. A statistical analysis using ANOVA on the results of Plate A determined that the current influences notch and HAZ depths, but the head speed did not or did so minimally. However, the interaction between amperage/current and head speed was statistically significant. This interaction indicated that amperage/current work together in a synergistic manner with head speed to cause aggressive marking conditions and deeper notches and HAZ. For example, high head speed (250 in/min) and high amperage/current (15 A) caused damaging conditions similar to medium amperage (13 A) and low head speed (100 in/min). Figure 3-5 illustrates this interaction by the diagonal pattern across the diagram showing that the notch and HAZ depths did not increase or decrease linearly with linear changes in current and writing speed – highlighting the interaction effect. The interaction effect only resulted in a statistically significant change in notch and HAZ depths for a change in head speed, between the 13 and15 A settings.

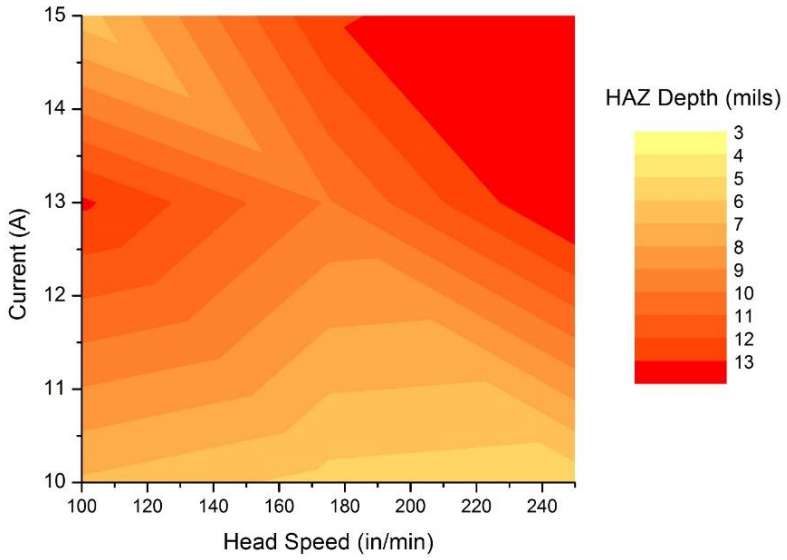

Figure 3-5. Contour plot indicating trends in absolute values of HAZ depth as a function of current and head speed (Plate A).

To elucidate the difference between the 13 and 15 A settings (i.e., the higher current settings, representing the most aggressive conditions), Plate B and C were marked in random order at varying head speeds using these two levels of current (the data are shown in Figure 3-6). The random order allowed for the removal of external effects associated with time or marking order, such as machine efficiency or inefficiency as a function of time. Twenty notch and HAZ depth measurements were taken at each combination of current and head speed. Using an ANOVA with a p value of 0.05, the notch and HAZ depths in plate B and C showed no statistically significant difference between 13 and 15 A, similar to the results of plate A. Additionally, writing/head speed did not have a statistically significant effect on notch and HAZ depths.

Through the above analysis, it was determined that certain write speeds can combine with certain marking currents to create an isolated zone of high HAZ depth. This trend is clearly seen in the contour plots of Figure 3-6 below, where the notch and HAZ depth is largest at different levels of head speed, depending on the level of amperage. This interaction effect is shown by the trend of notch and HAZ depths diagonally across Figure 3-6. An additional observation was made during these tests that indicated a possible plate-to-plate dependence of HAZ depth since the data in Figure 3-6 (left) has a different pattern than the data in Figure 3-6 (right).

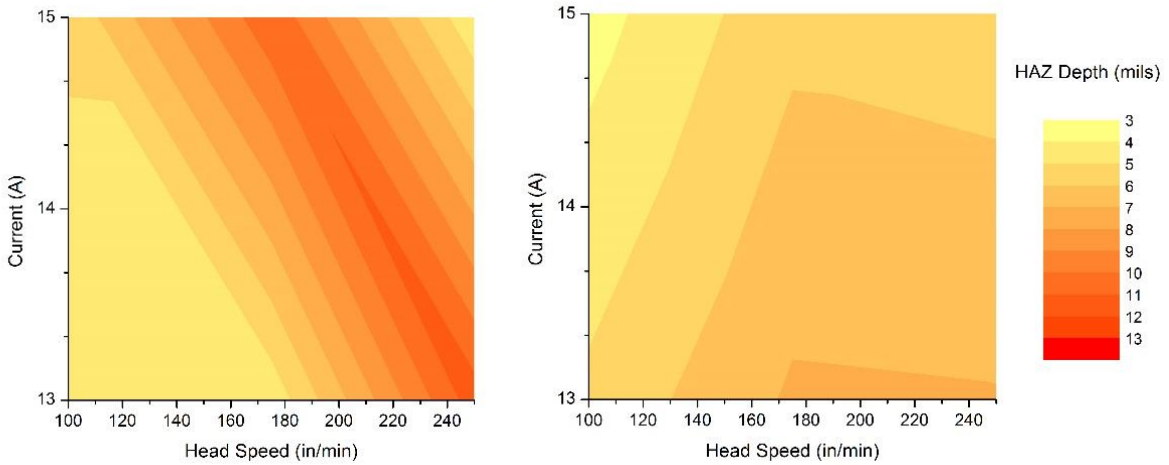

Figure 3-6. Contour plot indicating trends in absolute values of notch and HAZ depths as a function of current and head speeds of Plate B (left) and Plate C (right).

3.1.2 Comparison of Notch and HAZ Depths Among Plates

To study the variability of the notch and HAZ depth from plate-to-plate, a t-test was used to compare the average notch and HAZ depths and standard deviations of plates marked at the same condition (15 A and 250 in/min). Results of notch and HAZ depth for plates A, B and C are shown in Figure 3-7. Since the notch and HAZ depths of plates B and C are statistically equivalent, they are combined into one group and then compared with A. Table 3-1 shows the t-test statistics for plate B and C demonstrating that they are not statistically different. The statistical difference between three conditions is summarized below in Table 3-2 with a significance level of p set at 0.05 for the t-test.

Table 3-1. Descriptive t-test statistics with a significance level of p set at 0.05.

Plate	HAZ Depth Mean (mil)	Std.Dev (mil)	P-value	Difference Statistically Confirmed
B	3.58	1.34	0.13	No
C	2.35	2.03		

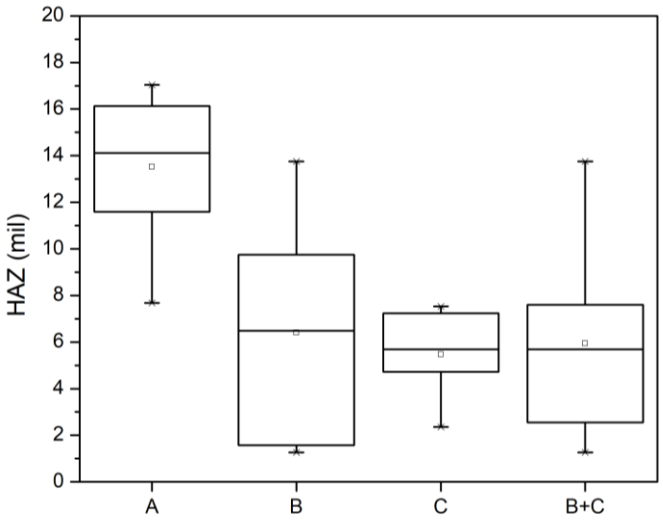

Figure 3-7. Comparison of HAZ depth among plate A, B and C (B+C) for 15 A and 250 in/min. The box indicates the interquartile range. Error bars represent 1st (upper) and 3rd (lower) quartile.

Table 3-2. T-test results of the plates showing plate A having a statistically different notch and HAZ depth relative to plates B+C

Marking Parameters	Plate A HAZ Depth Mean ± Std.Dev (mil)	Plate B+C HAZ Depth Mean ± Std.Dev (mil)	Difference Statistically Confirmed	P-value
15 A and 250 in/min	13.5 ± 3.1	8.5 ± 5.4	Yes	0.003
13 A and 250 in/min	14.3 ± 4.9	5.4 ± 3.2	Yes	0.000
13 A and 100 in/min	13.2 ± 2.2	5.2 ± 4.0	Yes	0.000

In order to determine the possible causes of variability in notch and HAZ depth among the plates using same parameters, hardness and grain size measurements on plate A, B and C were done. Measurements of grain size were taken using the mean lineal intercept method per ASTM E112 (ASTM 2013). In Figure 3-8, a representative micrograph of plate C is shown. Micrographs of plates A and B are shown in the appendix section of this report and do not show any differences compared to plate C. The white areas are the pro-eutectoid ferrite phase and the dark areas represent pearlite. The grain size number was the same for the three plates and was confirmed to be within specifications for grade 50W for all plates studied. The grain size of each plate versus the maximum 50W grain size is summarized in Table 3-3. Hardness measurements on all three plates were taken using a Vickers indenter and the results of plates A, B and C were determined to be statistically equivalent. The hardness results of each plate are summarized in Table 3-4.

From the above similar hardness and grain size results we can conclude that the variability in notch and HAZ depth among the plates using same marking parameters is not due to difference in hardness or microstructure among the plates. Furthermore, both grain size and hardness values complied with the minimum standards established for the structural steel used in this study. This indicates that each plate was metallurgically equivalent.

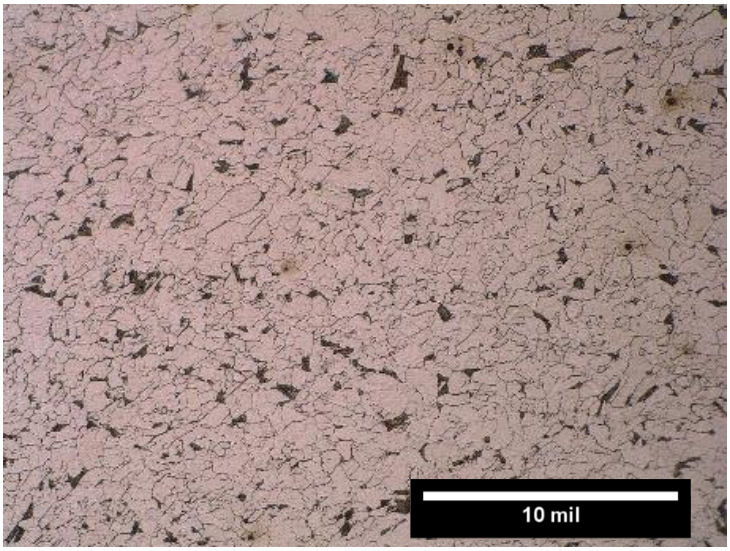

Figure 3-8. Micrograph of Plate C (500X).

Table 3-3. Grain sizes of plates A, B, C and 50W weathering steel.

	Plate A	Plate B	Plate C	50W Nominal (standard)
Grain Size(mil)	0.64 ± 0.08	0.59 ± 0.05	0.57 ± 0.12	2.55 max
Grain Size Number #	9	9	9	5 minimum

Table 3-4. Average Vickers hardness values of plates A, B, and C, using a 500-gram force.

	Plate A	Plate B	Plate C
Hardness (Vickers)	187.2 ± 5.1	181.7 ± 5.5	186.4 ± 5.2

Another source of notch and HAZ depth variability among plates marked with the same conditions is the planarity of the plates. A perfectly planar plate ensures that there is more consistent contact with the plasma arc during marking, hence resulting in a more

consistent and deeper notch and HAZ depths. This is supported by visual observation during the marking process. Plate B and C were observed to have intermittent and inconsistent contact with the plasma during marking. However, Plate A, which was much more planar, visibly to the eye, did not experience this effect. This difference in planarity can create plate-to-plate differences in the notch and HAZ depths.

3.1.3 Changes in Notch and HAZ Depth Along the Plasma Marks

Another factor to consider during the marking process is the change in mark morphology along the length of the plasma mark. A comparison of two marks is shown below in Figure 3-9 at differing settings. The top and bottom images illustrate the effect on the plasma mark at 13 A and 175 in/min and at 10 A and 250 in/min respectively. The marking depth and visibility changes as a function of distance and with the marking condition. The beginning of each plasma mark has a larger depth leading to a “trail-off” effect towards the end

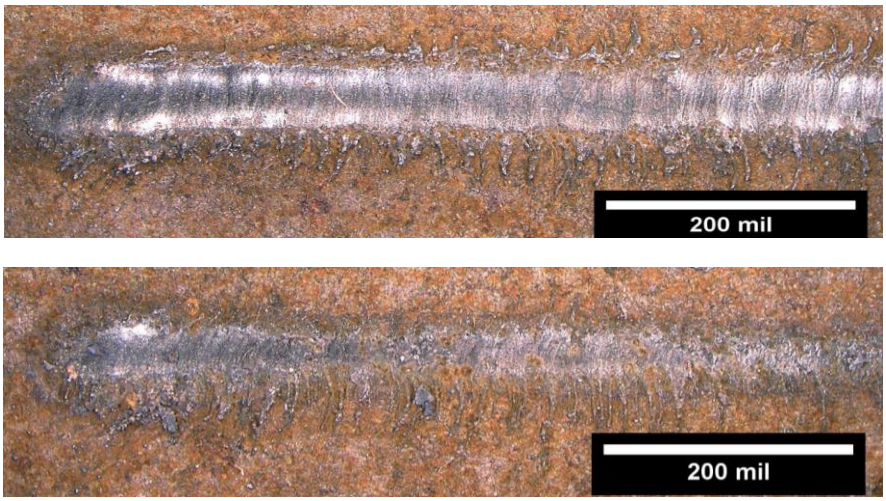

Figure 3-9. Plasma marks at 13 A and 175 in/min setting (above) and 10 A and 250 in/min setting (below)

Figure 3-10 provides quantitative data indicating that the HAZ decreases as a function of marking length (i.e. distance along the mark from the beginning to the end). This effect was statistically signification as confirmed through a one-way ANOVA (p-value = 0.05). The beginning of the mark contains the largest HAZ depth and is statistically different than the HAZ depths further along the mark.

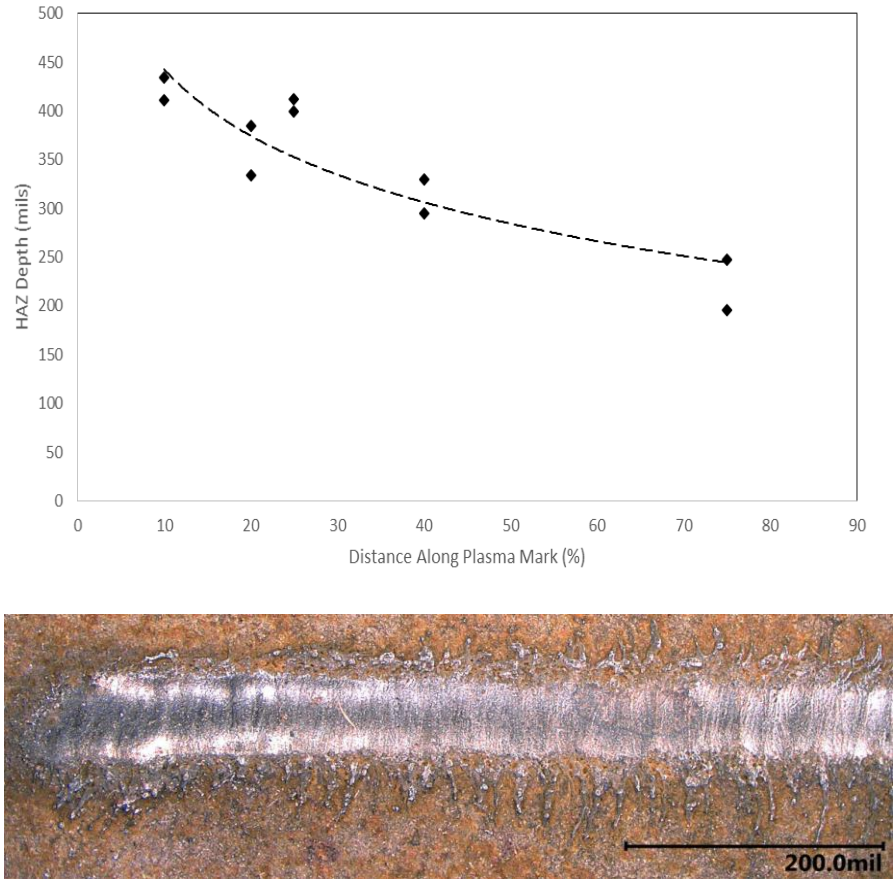

Figure 3-10. HAZ depth trails off as mark continues (above) and associated distances (below). Marked at 15 A and 250 in/min

3.2 Mechanical Characterization

3.2.1 Tensile Testing of Marked Specimens

A representative stress vs. strain curve is shown below in Figure 3-11 for one of the specimens from plate 3. This sample was marked at the 15 A and 75 in/min setting. The yield strength was higher than the 50 ksi minimum required for the steel grade, and consistent among all samples tested. Both the marked and unmarked samples experienced ductile failure, which is expected for an HSLA steel. All specimens failed in the gage section and away from the notch, effectively testing bulk properties.

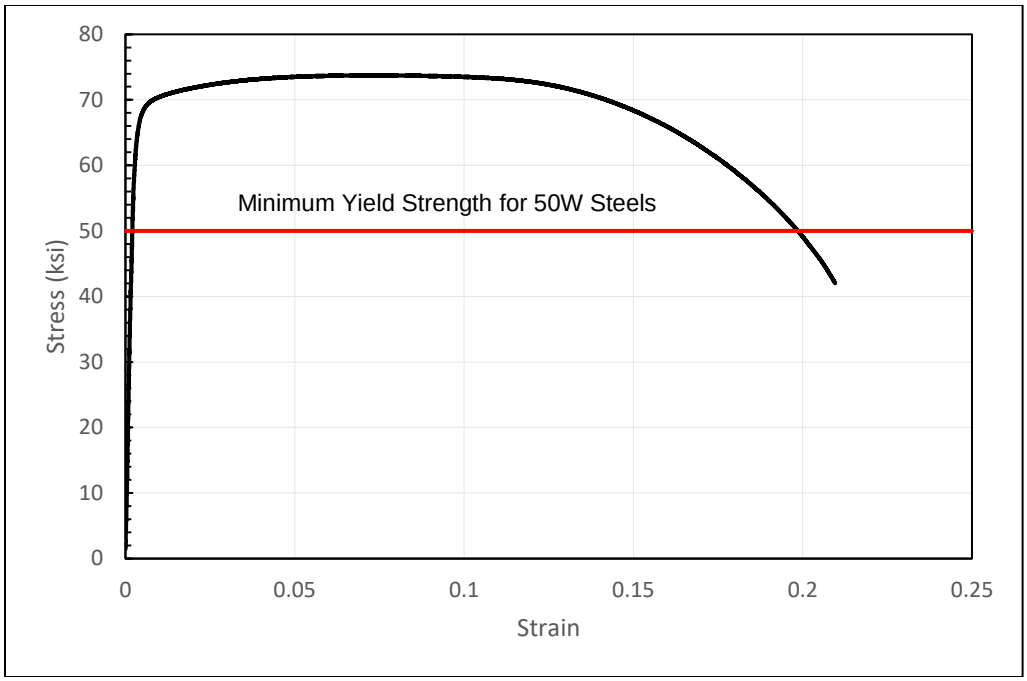

Figure 3-11. Representative stress versus strain curve illustrating the mechanical properties for bulk failure of tensile specimen.

This result indicates that there is a minimal effect of the marking on the tensile behavior of the material at the marking condition of 15 A. Since, none of the samples experienced failure at the notches, and given that the 15 A setting creates a much larger notch and HAZ depth and subsequently a higher stress intensity factor, it was determined that no tensile testing of the less aggressive 10 A setting was necessary.

To characterize any variation in mechanical properties across the plate, the yield and ultimate tensile strengths were analyzed using ANOVA in the Minitab software and it was determined that there was no statistically significant difference in strength properties as a function of the specimen location on the plate.

3.2.2 Fatigue Life of Specimens Marked at Different Parameters

In order to study the effect of plasma marking on the service life of the specimens, fatigue testing on samples marked with a current of 15 A at 75 in/min (33 samples) and 10 A at 150 in/min (35 samples) was done. For the 15 A at 75 in/min marking condition, 6 samples out of 33 experienced failure at the plasma mark, and 3 of these 6 samples failed beneath the minimum fatigue (Figure 3-12). The minimum fatigue life obtained was 107,458 cycles which is considerably lower than the minimum fatigue lifetime required for 50W structural steel bars represented by the black diagonal line in Figure 3-12. For the 10 A at 150 in/min setting, the samples do not seem to be weakened by the

plasma mark (e.g., no samples failed below the AASHTO Category A limit). The plasma mark appears to have introduced a small flaw that caused the failure to occur at the location of the mark in 2 of the 34 specimens, but all 34 met the AASHTO A standard surpassing the minimum fatigue life requirement.

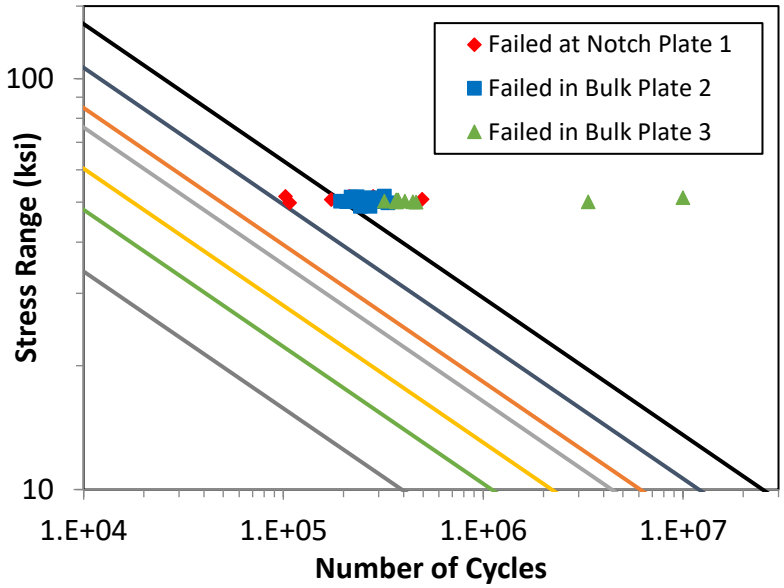

Figure 3-12. Stress range as function of number of cycles for the plate marked at 15 A, 75 in/min. Points in red represent samples that failed at the plasma mark. The fatigue data is overlaid on the AASHTO standard, where the black line represents Category A guidelines .

To highlight the relation between the cycles to failure, location of the failure and HAZ depth for both marking conditions, HAZ depths were plotted against the cycles to failure as shown in Figure 3-13. This plot reveals that all of the failures that occurred at the mark were due to the presence of a HAZ larger than 14 mils. This zone is highlighted in red. Although marks up to 17 mils were correlated with samples that did meet the minimum fatigue life, the 14 mils limit is used as a conservative measure. This scatter of the fatigue life values is largely a result of the stochastic nature of fatigue (Boardman 1990). As shown in the results from section 3.1 marking setting of 13 and 15 A are capable of creating HAZ larger than 14 mils. Thus, these results indicate that a limitation to the 10 A setting is recommended.

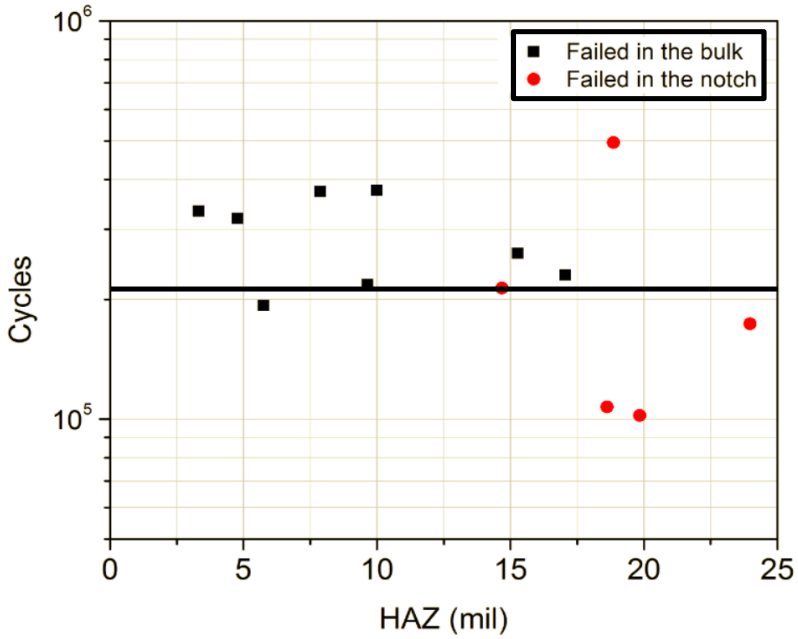

Figure 3-13. Scatter plot of cycles to failure vs. HAZ depth. Points in red indicate samples that failed at the HAZ. Light red zone indicates the range of HAZ depths that could cause premature to minimum fatigue life failure.

In order to have a statistically-significant amount of data to establish safe parameters for marking, fatigue testing on 108 samples marked using a current of 10 A at three different head speeds was done. Figure 3-14 shows the fatigue testing results for: (a) compiled data for all the samples tested at three head speeds, (b) plates 9 and 10 marked at 75 in/min, (c) plates 4,5 and 6 marked at 150 in/min and, (d) plates 7 and 8 marked at 250 in/min. All the samples that failed at the mark are plotted as orange data points. Most of the samples marked at 250 in/min speed, Figure 3-14(d), failed at the plasma mark. However, three of those samples (plate 7) failed below the minimum fatigue life for category A rolled structural steel bar (AASHTO 2015). Table 3-5 shows the mean value of the fatigue life for each plate and the respective marking parameters. By comparing the data obtained from specimens marked at different head speeds, there was not a statistically-significant difference in the fatigue life of the specimens.

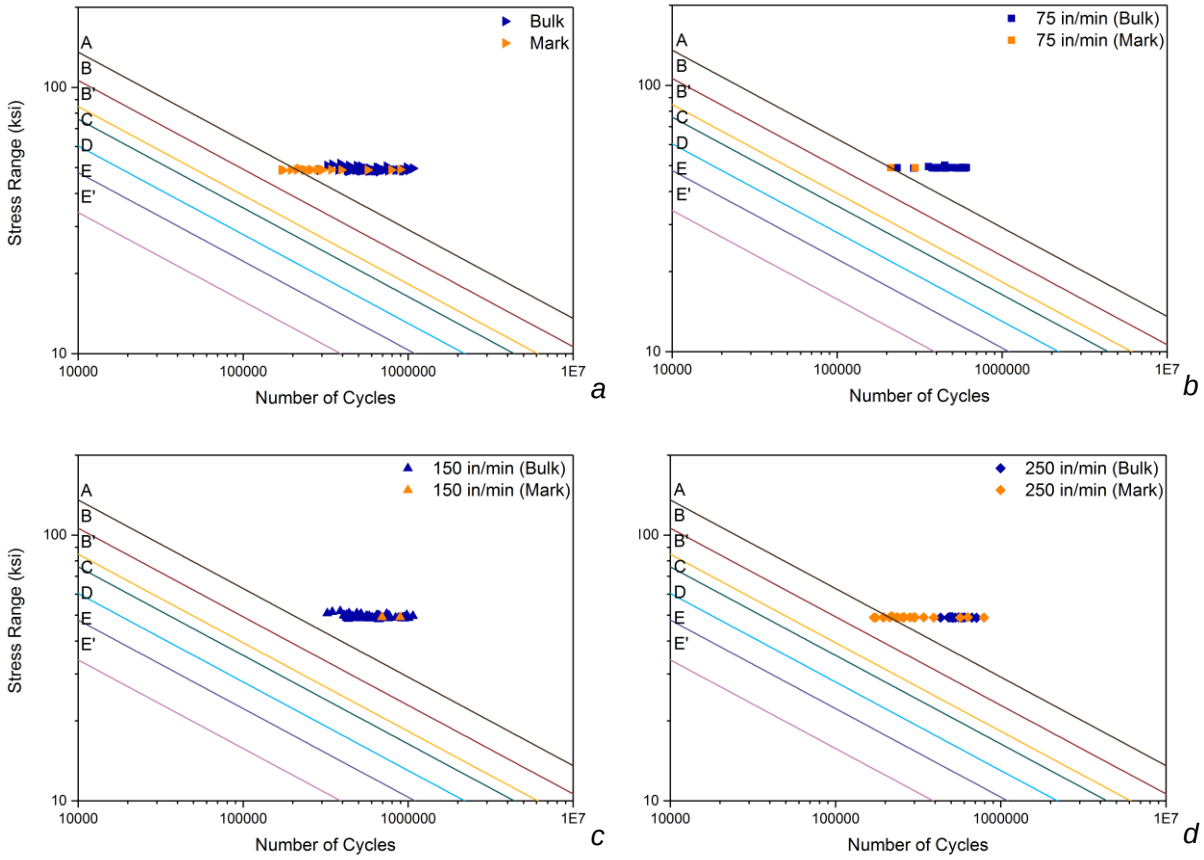

Figure 3-14. Stress range vs. cycles to failure for 50W samples marked at the 10-A condition. (a) Data from all plates marked at three different head speeds, (b). Plates 9 and 10 marked at 75 in/min, (c) Plates 4, 5, and 6 marked at 150 in/min, and (d) Plates 7 and 8 marked at 250 in/min. In every plot, the samples that failed in the plasma mark are identified by the color orange.

There is a significant difference in the average number of cycles between plate 7 and 8, which indicates that the fatigue life may be affected by plate-to-plate differences, such as plate planarity. This was expected since previous ANOVA analysis confirmed the statistical difference between the HAZ depths between plates despite the same marking parameters.

Table 3-5. Average number of cycles to failure of the tested plates and marking conditions.

Plate	Head speed (in/min)	Average No. Cycles to Failure		Standard Deviation	
4	150	621,247	461,177	236,357	99,678
5		664,999		193,834	
6		575,316		105,422	
7	250	297,788	620,520	159,761	186,818
8		531,322		97,669	
9	75	471,726	417,891	90,029	175,513
10		444,385		111,385	

3.3 Fatigue Life Probability Plots

Most of the tested samples failed above the minimum fatigue life for AASHTO category A for a rolled structural steel bar. In order to determine the probability of a specimen failing below the minimum life according to the AASHTO guidelines, a probability plot with the fatigue data was made.

After determining that the data best fits a normal distribution by analyzing the Anderson – Darling statistic and p-value across many different possible distributions, a probability graph for each plasma head speed was plotted in Figure 3-15. This analysis allows for a comparison of the fit of the data to the normal distribution and the percentage of samples that are likely to fail below the minimum fatigue life of 175000 cycles at a stress range of 50 ksi (i.e., AASHTO category A) as shown in Figure 3-15 by the red dotted line.

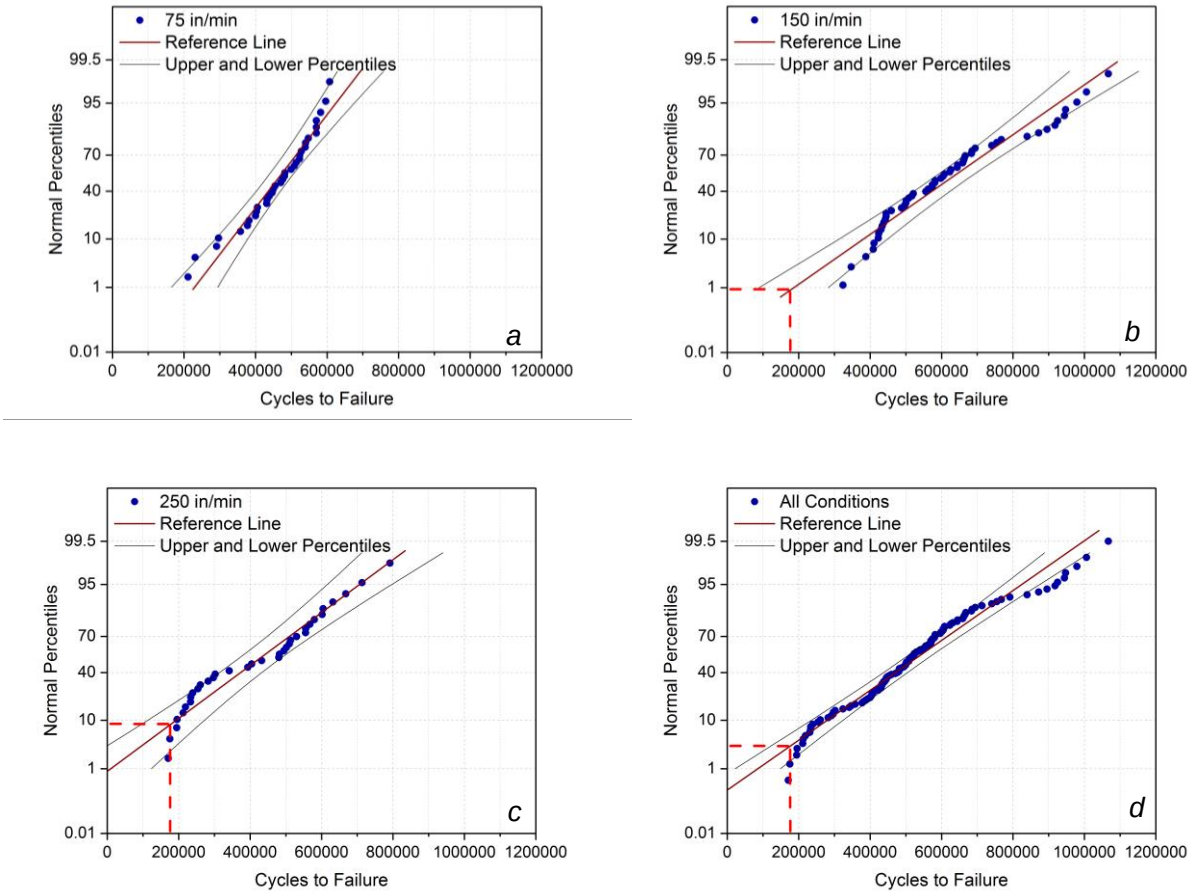

Figure 3-15. Normal distribution plot showing probability of failure below minimum fatigue life of 175,000 cycles for samples marked at 10 A and head speeds of (a) 75, (b) 150, (c) 250 in/min, and (d) all conditions. The minimum life according to the AASHTO guidelines is indicated by the red dotted line.

As can be seen in Figure 3-15, with the number of failed samples below the fatigue limit, there is a low probability of the samples failing below the AASHTO minimum fatigue lifetime for 50W steel category A. With a 0.05 confidence level, none of the samples marked at 10 A and a head speed of 75 in/min are likely to fail below the minimum (Figure 3-15a). While, there is 0.9% and 8.4% probability that any sample marked at 150 and 250 in/min, respectively, will fail below the AASHTO minimum fatigue lifetime for 50W steel category A. As demonstrated in Section 3.1.1, plasma marks made at 10 A with different head speeds are not statistically significantly different. By plotting the cycles of all the samples marked at 10 A and different head speeds on a single plot, there is only a 3.2% probability of the sample failing below the AASHTO minimum fatigue lifetime for 50W steel, category A. The mean fatigue life is 518,351 cycles to failure with a standard deviation of 186,239 cycles to failure.

4 Final Safety Guideline Result

The 10-A condition creates a visible and robust mark that can be used for surface marking. This study has shown that this technology has the potential to be used as a marking technique. It was determined that there is only a 3.2% probability that a sample marked with plasma at a current of 10 A and 75-250 in/min speed will fail below the AASHTO minimum fatigue lifetime for 50W steel. The minimum fatigue life obtained was 170,767 cycles which is considerably close to the minimum fatigue lifetime required for 50W structural steel bars.

5 Summary

- Current was shown to have an effect on HAZ depth; head speed was shown to create no change in the HAZ depth in a consistent or predictable manner.
- Current only created a statistically significant difference in HAZ depth between 10 and 13 A, and 10 and 15 A. The difference between 13 and 15 A is not statistically significant.
- The possible depths that the HAZ can reach can be grouped into two distinct sets of marking parameters: 10 A and 13/15 A.
- The setting of 15 A, is not recommended for future use as a marking setting due to the significant number of samples that failed bellow the AASHTO minimum fatigue lifetime for 50W steel. Furthermore, since both the 13- and 15-A settings can cause damage at similar levels, it is recommended that these current/amperages be avoided for marking of 0.5” 50W steels.
- The setting of 10 A, is recommended for future use as a marking setting. It was determined that there is only a 3.2% probability that a sample marked with plasma at a current of 10 A will fail below the AASHTO minimum fatigue lifetime for 50W steel.
- Plate-to-plate variability was a significant factor affecting the value of the notch and HAZ depth as the plates are not perfectly planar. The most planar plates resulted in the largest HAZ depths. This is the reason that all the HAZ depths on Plate 7 were higher than any others seen at 10 A and that failures occurred before the necessary fatigue lifetime.

References

AASHTO. 2015. *LRFD Bridge Design Specifications*. Washington, D.C.: AASHTO.

ASTM. 2009. “Standard Test Methods for Tension Testing of Metallic Materials.” *ASTM International* E8/E8M − 1:1–27. https://doi.org/10.1520/E0008.

ASTM. 2013. “Standard Test Methods for Determining Average Grain Size.” *ASTM International* ASTM E112:1–28. https://doi.org/10.1520/E0112-13.1.4.

ASTM. 2016. “Standard Specification for Structural Steel for Bridges.” *ASTM International* A70–A709M:1–8. https://doi.org/10.1520/A0709.

Bain, Kenneth R., and David S. Miller. 2000. “Fatigue Crack Growth Threshold Stress Intensity Determination via Surface Flaw (Kb Bar) Specimen Geometry.” *Fatigue and Fracture Mechanics* 31:445–56.

Boardman, Bruce. 1990. “Fatigue Resistance of Steels.” In *Properties and Selection: Irons, Steels, and High Performance Alloys*, 1:673–88. https://doi.org/10.1361/asmhba0001038.

Faulkner, Luke. 2011. “Automating Layout in Steel Fabrication.” *Modern Steel Construction*, 2011.

Kesler, M.S., P. Feldtmann, E.S. George, S.M. Duke, and M.V. Manuel. 2016. “Effect of Plasma Marking on the Fatigue Properties of Grade 50W Steel.” *Journal of Materials in Civil Engineering* 28 (9):3–8. https://doi.org/10.1061/(ASCE)MT.1943-5533.0001588.

Appendix A

A.1 Project Schedule

Table A-1. Project Schedule.

Deliverable # / Description (Associated Task)	Anticipated date of deliverable submittal	TO BE COMPLETED BY RESEARCH CENTER (actual submittal date)
Kickoff Meeting	October 2017	
Deliverable 1 – A written report that contains statistically relevant fatigue data outlining the conditions that are safe for marking, while also remaining clearly discernable. (Task 1)	October 2017	
Deliverable 2A – Draft final report containing recommendations regarding testing parameter ranges, ranges for nominal and maximum marking depths. (Task 2)	November 2017	
Deliverable 2B – Closeout Teleconference (Task 2)	January 2017	
Deliverable 3 – Final Report (Task 3)	February 2018	

A.2 Plates Micrograph

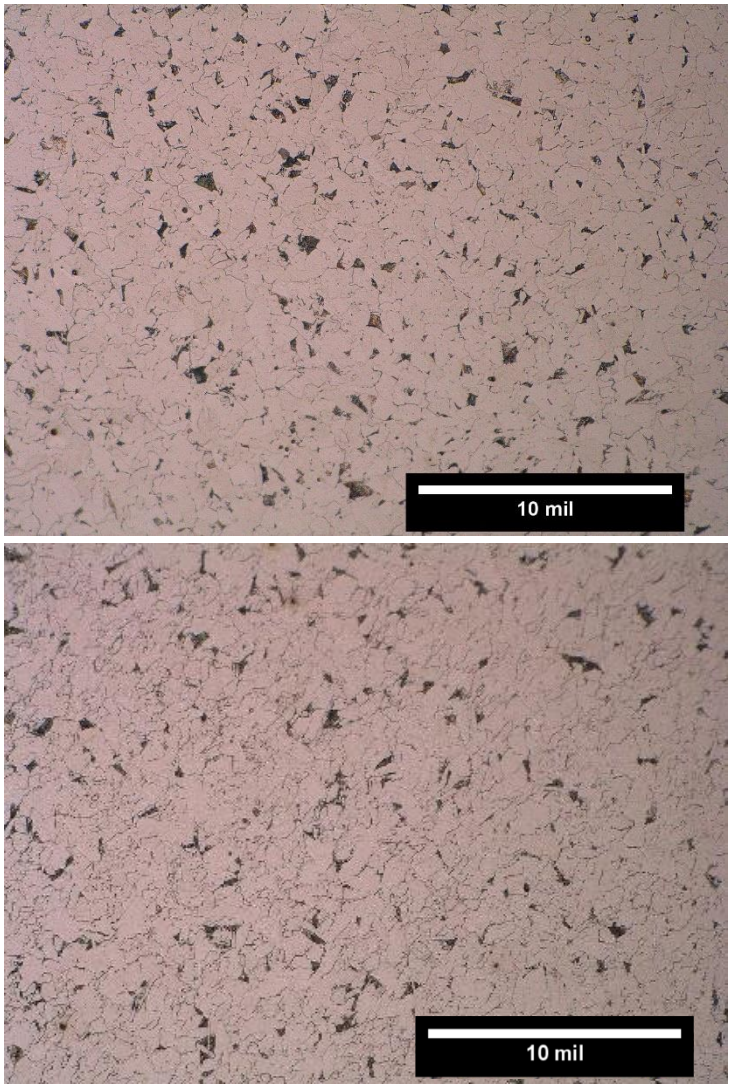

Figure A-16. Micrograph at 500x for plate A (top), and plate B (bottom).

A.3 Mechanical Testing Results

Table A-2. Ultimate tensile strength and yield strength values for specimens from plate 1 and 3.

Plate	Position on Plate	Sample Number	Amperage (A)	Head speed (in/min)	UTS (ksi)	Yield Strength (ksi)
1	Top	1	13	75	73.1	68
1	Top	2	13	75	73.7	68
1	Top	3	13	75	73.75	67.5
1	Bottom	4	10	75	74.3	67
1	Bottom	5	10	75	74.7	68
1	Bottom	6	10	75	68.8	62
1	Bottom	8	10	75	74.2	67
1	Bottom	9	10	75	73.5	64
1	Bottom	1	13	75	74.6	69
1	Bottom	2	13	75	74.6	69
3	Bottom	1	15	75	73.7	69.5
3	Bottom	2	15	75	73.5	67
3	Bottom	3	15	75	72.9	70
3	Bottom	4	15	75	73.4	68
3	Bottom	5	15	75	73.8	68.5
3	Bottom	6	15	75	73.7	69

Fatigue Data

Current: 15 A

Table A-3. Cycles to failure (fatigue life) of specimens from plates 1-3.

Plasma Mark	Mark Failure	Plate #	Delta Sigma(ksi)	Cycles to Failure
Yes	Yes	1	50.8	173,550
Yes	Yes	1	49.8	107,458
Yes	Yes	1	51.7	281,076
Yes	Yes	1	51.7	213,374
Yes	Yes	1	51.6	102,312
Yes	Yes	1	50.9	494,945
Yes	No	2	51.1	261,330
Yes	No	2	49.8	333,420
Yes	No	2	50.1	230,221
Yes	No	2	50.2	312,515
Yes	No	2	48.9	242,543
Yes	No	2	51.8	319,642
Yes	No	2	50.6	277,796
Yes	No	2	50.4	261,107
Yes	No	2	50.2	207,037
Yes	No	2	50.7	227,931
Yes	No	2	48.9	271,000
Yes	No	2	51.3	276,568
Yes	No	2	50.6	300,696
Yes	No	2	51.6	233,581
Yes	No	2	51.4	217,908
Yes	No	2	50.3	193,229
Yes	No	3	51.3	10,000,000
Yes	No	3	50.6	375,690
Yes	No	3	50.5	372,809
Yes	No	3	50.3	405,907
Yes	No	3	50.3	320,620
Yes	No	3	50.1	444,122
Yes	No	3	50.1	367,201
Yes	No	3	50.1	3,355,864
Yes	No	3	50.1	367,661
Yes	No	3	50.6	366,878
Yes	No	3	50.0	461,405

Current: 10 A

Table A-4. Cycles to failure (fatigue life) of specimens from plates 4-10.

Plasma Mark	Mark Failure	Plate #	Delta Sigma(ksi)	Cycles to Failure
Yes	No	4	50.1	979,103
Yes	No	4	50.6	517,413
Yes	No	4	49.1	944,196
Yes	No	4	48.9	839,673
Yes	No	4	50.9	323,951
Yes	No	4	48.8	444,860
Yes	Yes	4	49.2	895,692
Yes	No	4	49.7	1,067,318
Yes	No	4	50.1	445,181
Yes	No	4	51.7	387,953
Yes	No	4	51.4	346,889
Yes	No	4	50.8	438,192
Yes	No	4	49.9	659,528
Yes	No	4	48.9	683,850
Yes	No	4	50.8	488,245
Yes	No	4	50.1	408,767
Yes	No	4	49.8	666,675
Yes	No	4	50.0	644,964
Yes	No	5	49.7	411,254
Yes	No	5	48.7	508,551
Yes	No	5	48.7	574,615
Yes	No	5	49.5	556,068
Yes	No	5	48.4	433,884
Yes	No	5	48.7	608,220
Yes	No	5	49.7	581,977
Yes	No	5	48.9	1,006,200
Yes	No	5	50.6	740,894
Yes	No	5	48.9	424,312
Yes	No	5	49.1	685,504
Yes	No	5	48.6	917,908
Yes	No	5	48.7	755,119
Yes	No	5	49.8	767,702
Yes	No	5	49.0	925,168
Yes	No	5	49.1	694,580
Yes	No	5	48.6	947,287
Yes	No	6	48.7	626,381
Yes	No	6	49.1	501,089
Yes	No	6	48.3	663,502
Yes	No	6	49.6	442,540

Plasma Mark	Mark Failure	Plate #	Delta Sigma(ksi)	Cycles to Failure
Yes	No	6	49.6	459,926
Yes	No	6	49.7	500,151
Yes	No	6	49.7	562,728
Yes	No	6	49.8	496,920
Yes	No	6	50.1	422,888
Yes	No	6	48.6	581,119
Yes	No	6	48.9	661,491
Yes	No	6	48.9	872,039
Yes	No	6	48.6	520,715
Yes	No	6	48.8	598,049
Yes	No	6	48.8	623,353
Yes	No	6	48.6	644,077
Yes	No	6	49.0	573,911
Yes	No	6	49.0	604,802
Yes	Yes	7	49.0	233,271
Yes	Yes	7	49.1	282,316
Yes	Yes	7	49.0	393,335
Yes	Yes	7	49.0	233,674
Yes	Yes	7	49.6	219,045
Yes	Yes	7	49.1	212,572
Yes	Yes	7	49.0	297,553
Yes	Yes	7	49.0	239,115
Yes	Yes	7	49.0	194,484
Yes	Yes	7	48.9	175,361
Yes	Yes	7	49.1	195,836
Yes	Yes	7	49.1	341,666
Yes	Yes	7	49.0	567,457
Yes	Yes	7	49.0	791,435
Yes	Yes	7	49.0	170,767
Yes	Yes	7	49.0	253,975
Yes	Yes	7	49.1	260,528
Yes	No	8	49.0	432,149
Yes	No	8	49.1	502,045
Yes	No	8	49.1	302,529
Yes	No	8	49.2	494,864
Yes	No	8	48.9	513,477
Yes	No	8	49.0	482,192
Yes	No	8	49.2	404,430
Yes	No	8	49.1	555,849
Yes	No	8	48.9	580,197
Yes	No	8	49.0	555,427
Yes	No	8	49.0	602,023

Plasma Mark	Mark Failure	Plate #	Delta Sigma(ksi)	Cycles to Failure
Yes	No	8	49.1	510,201
Yes	No	8	0.0	480,261
Yes	No	8	49.0	604,674
Yes	No	8	49.0	530,140
Yes	No	8	48.9	713,357
Yes	Yes	8	49.2	631,831
Yes	No	8	49.0	668,152
Yes	No	9	48.9	400,018
Yes	No	9	49.2	499,574
Yes	No	9	49.1	528,318
Yes	No	9	49.1	381,914
Yes	No	9	49.6	358,268
Yes	No	9	49.1	432,385
Yes	No	9	49.2	582,400
Yes	No	9	49.0	438,436
Yes	No	9	49.1	402,968
Yes	No	9	49.2	570,369
Yes	No	9	49.1	607,587
Yes	No	9	49.1	481,275
Yes	No	9	0.0	405,496
Yes	No	9	48.9	570,326
Yes	No	9	48.9	291,134
Yes	No	9	49.5	446,344
Yes	No	9	49.2	570,369
Yes	No	9	49.0	523,885
Yes	No	10	49.1	513,737
Yes	Yes	10	49.1	297,012
Yes	No	10	49.0	377,521
Yes	No	10	49.1	508,328
Yes	No	10	49.0	596,632
Yes	No	10	49.0	523,363
Yes	No	10	49.1	476,104
Yes	No	10	49.1	231,141
Yes	No	10	48.9	454,711
Yes	Yes	10	49.1	211,529
Yes	No	10	49.1	470,830
Yes	No	10	50.2	449,103
Yes	No	10	49.1	482,104
Yes	No	10	49.1	548,040
Yes	No	10	48.9	538,865
Yes	No	10	49.2	431,132